Applied Physics Letters ARTICLE scitation.org/journal/apl

Three-point I–V spectroscopy deconvolves region-specific degradations in LDMOS transistors

Cite as: Appl. Phys. Lett. **119**, 122102 (2021); doi: 10.1063/5.0058477
Submitted: 30 May 2021 · Accepted: 1 September 2021 ·
Published Online: 21 September 2021

Yen-Pu Chen,[1] Bikram K. Mahajan,[1] Dhanoop Varghese,[2] Srikanth Krishnan,[2] Vijay Reddy,[2] and Muhammad A. Alam[1,a)]

AFFILIATIONS

[1]Department of ECE, Purdue University, West Lafayette, Indiana 47906, USA
[2]Texas Instruments Inc., Dallas, Texas 75043, USA

[a)]Author to whom correspondence should be addressed: alam@purdue.edu

ABSTRACT

Unlike traditional logic transistors, hot carrier degradation (HCD) in power transistors involves simultaneous and potentially correlated degradation in multiple regions. One must deconvolve and characterize the voltage- and temperature-dependence of these region-specific degradations to develop a predictive HCD model of power transistors. Unfortunately, power transistors' doping and geometrical complexities make it challenging to use traditional defect-profiling techniques, such as charge-pumping or gated-diode methods. This Letter uses a physics-based tandem-FET model of an Laterally Diffused MOS (LDMOS) transistor to develop a "three-point I–V spectroscopy" technique that uses the time-evolution of three critical points of the measured I–V characteristics to extract mobility and threshold voltage degradations in the channel and drift regions. This innovative approach should generalize to other configurations of the LDMOS transistor as well.

Unlike conventional logic transistors, power transistors are used in high-temperature and high-power applications. Laterally Diffused MOS (LDMOS) is widely used in smart power ICs, power amplifiers, automotive applications, etc., due to its CMOS compatibility and high efficiency. This class of power transistors uses specialized doping profiles and a relatively long drift region to suppress the peak electric field within the device. Many groups have also proposed new structures to enhance its breakdown voltage and reduce on-resistance.[1,2] Despite careful design (and like all other power transistors), an LDMOS suffers from significant hot carrier degradation. The energetic carriers break Si–H and Si–O bonds[3] at the Si/SiO_2 interface, which in turn degrade the carrier mobility ($\Delta\mu$) and increase the threshold voltage (ΔV_{th}). Careful experimental and theoretical analyses[4] suggest that the complex doping profiles of power transistors create multiple hotspots, characterized by the high surface electric field and impact ionization. Therefore, unlike traditional logic transistors, the overall hot carrier degradation (HCD) degradation is attributed to several localized HCD along the gate/oxide interface.[5–7]

Traditionally, HCD in a power transistor has been characterized by metrics originally developed for *logic transistors*, such as $\Delta I_{D,lin}$, ΔR_{on}, $\Delta G_{m,max}$, ΔV_{th}. The lifetime of logic transistors can be predicted by time kinetics of degradation in a phenomenological expression, e.g., $At^n/(1+Bt^n)$,[8] where A and B are voltage- and temperature-dependent coefficients. The HCD in logic transistors occurs only in a region close to the drain; therefore, the classical models cannot capture the voltage dependent HCD of LDMOS transistors involving multiple degraded regions between the source and drain. One may obtain the localized HCD using multi-region charge pumping (CP) techniques, with pulse shapes tailored for the characteristic variation of threshold and flatband voltages across the device.[9–12] However, such techniques require a sophisticated setup and a separate set of experiments. Other groups have developed equivalent circuits to separate the transistor into several parts and adjusted the corresponding parameters to mimic the localized degradation.[13,14] The distinctive feature of the analytical model proposed in this paper is that it allows direct extraction of the critical transistor parameters from the characteristic points of the degradation spectrum. Specifically, we propose a straightforward methodology to analyze the region-specific HCD [in $\Delta\mu(\%)$] by the "three-point IV spectroscopy" technique. The technique is based on Si LDMOS, which is modeled as a "tandem-FET" structure to connect the parametric degradation of the individual FETs to the corresponding features of the I–V characteristics. The evolution of the critical elements is then mapped back to the region-specific HCD degradations. It is already known that the *full* I–V spectroscopy, supported by tandem-FET compact modeling, can quantify region-specific degradation in LDMOS transistors.[4] The key contribution of this paper is the

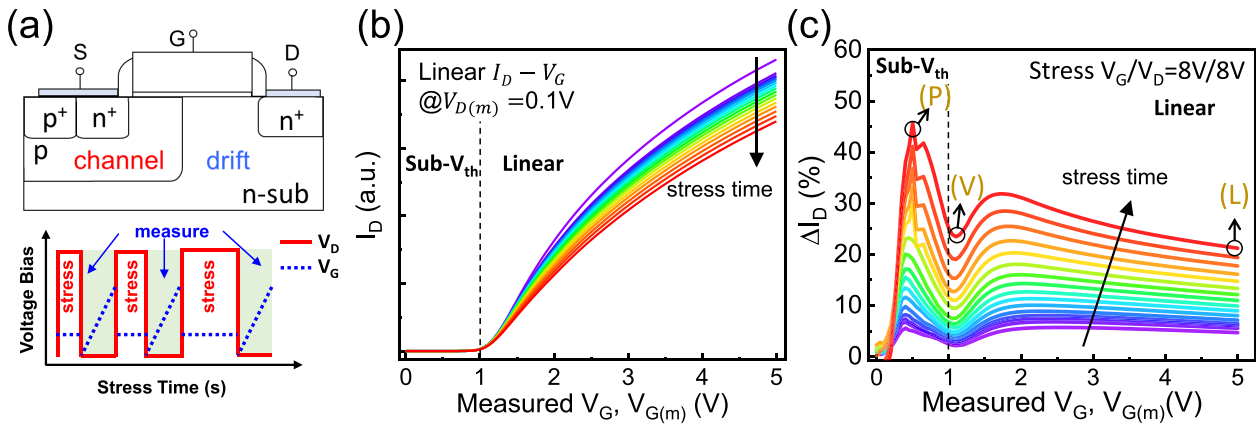

FIG. 1. (a) The schematic of the LDMOS used in the study and its HCD test illustration. Detailed device information can be found in the supplementary material. (b) The degradation of $I_D - V_G$ curves in measurement phases [indicated by (m)] after consecutive stress phases [indicated by (s)]. (c) The degradation spectrum is obtained from the data in (b). Three important $V_{G(m)}$ points: P (peak), V (valley), and L (linear) are labeled.

discovery that, tracking the degradation of three critical points on an $I_D - V_G$ curve, appropriately interpreted by the analytical formula, can preclude the use of a tandem-FET compact model and dramatically simplify the HCD characterization of LDMOS transistors.

The schematic of n-channel LDMOS transistors, fabricated on silicon wafers, is shown in Fig. 1(a). HCD tests are conducted by applying a constant voltage stress $[V_{D(s)}, V_{G(s)}]$ to generate interface defects and the consecutive $I_D - V_G$ measurements $[V_{D(m)}, V_{G(m)}]$ to quantify the defects generated. This stress-measure-stress sequence is shown at the bottom part of Fig. 1(a). For the illustrative example shown in Fig. 1, the stress conditions are $V_{D(s)} = 8$ V, $V_{G(s)} = 2, 4, 8$ V. During the measurement phase, $V_{D(m)}$ is kept at 0.1 V so that the measured current, sweeping of $V_{G(m)}$ from 0 to 5 V, is the linear current [Fig. 1(b)]. From each $I_D - V_G$ sweep, one can obtain $\Delta I_{D,lin}(t)$ and $\Delta V_{th}(t)$ after stress time t. (All I_D in this paper are obtained in the measurement phase.) Here, $I_{D,lin}$ is defined at $V_{G(m)} = 5$ V, $V_{D(m)} = 0.1$ V, and $\Delta V_{th}(t)$ is evaluated by determining the shift in $V_{G(m)}$ needed to keep the current constant at 10 μA (i.e., constant current method[15]) because $\Delta V_{th}(t)$ calculated using the maximum transconductance method might be contaminated by severe mobility degradation.[4]

After obtaining a series of $I_D - V_{G(m)}$ curves at successive intervals during stress, we plot the full differential $\Delta I_D - V_{G(m)}$ spectrum as a function of stress time t, see Fig. 1(c). Here, the degradation percentage,

$$\Delta I_D\left(V_{G(m)}, t\right) \equiv \frac{I_D\left(V_{G(m)}, t=0\right) - I_D\left(V_{G(m)}, t>0\right)}{I_D\left(V_{G(m)}, t=0\right)}, \quad (1)$$

is calculated at each $V_{G(m)}$ point. In other words, each degraded I–V curve ($t > 0$) is turned into the degradation ratio (in %) by point-by-point subtractions from their primitive current levels ($t = 0$). These characteristics behave like a degradation spectrum over $V_{G(m)}$ from the subthreshold region [$V_{G(m)} < 1$ V] to the linear region [$V_{G(m)} > 1$ V]. Interestingly, the spectrum shows a double peak behavior, corresponding to the subthreshold and linear regions, respectively. $\Delta I_D(\%)$ at three critical $V_{G(m)}$ points [$\Delta I_D^{(P)}(t)$, $\Delta I_D^{(V)}(t)$, and $\Delta I_D^{(L)}(t)$ in Fig. 1(c)] allow us to determine the three key quantities $\Delta\mu_{ch}$, $\Delta\mu_{dr}$, and ΔV_{th}^{ch} (noted in Fig. 2) by solving three analytical equations (to be derived below) corresponding to the P, V, and L points.

To develop the analytical theory of the three critical points, we first use a detailed numerical analysis of the tandem-FET compact model shown in Fig. 2. The insights from the numerical analysis pave the way toward simplified analytical expressions to quantify the degradation parameters. For a tandem-FET model, the p-type channel region can be represented by a normally off MOSFET, and the n-type drift region can be treated as a normally on MOSFET. Each transistor of this tandem-FET configuration is modeled by its BSIM6[16] representation with the corresponding V_{th}, μ, and geometric dimensions.[4] The source/drain series resistances are included in BSIM6 but are assumed not to degrade due to hot-carrier stress because the hot electrons are confined along the gate/oxide interface. The mobility degradation in the channel and drift regions ($\Delta\mu_{ch}$ and $\Delta\mu_{dr}$) and channel threshold voltage (ΔV_{th}^{ch}) have different impacts on the overall I–V degradation. We note that the compact model captures gate field-dependence of the mobility. However, $\Delta\mu$ in this paper refers to the degradation of low-field mobility, assuming the field dependent term of BSIM6 does not change after HCD. In general, modeling shows that ΔV_{th} in the drift region (ΔV_{th}^{dr}) does not affect the I–V characteristics significantly and, therefore, can be omitted for simplicity. A detailed calibration of this tandem-FET compact model to the experimental data can be found in the supplementary material.

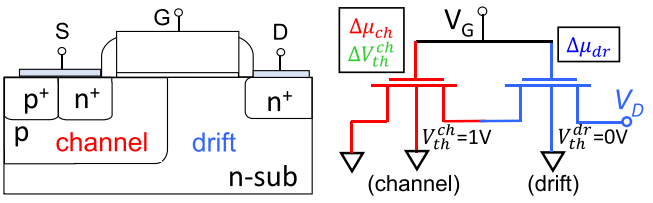

FIG. 2. The proposed tandem-FET compact model. The channel (ch) and the drift (dr) regions function individually as a MOSFET with different V_{th} and dimensions. Three adjustable degradation parameters are $\Delta\mu_{ch}$, ΔV_{th}^{ch}, and $\Delta\mu_{dr}$.

Now we can use the calibrated model to explore the I–V spectrum. Figure 3 shows how a typically measured I–V degradation data (black circle) can be fitted by adjusting $\Delta\mu_{ch}$, ΔV_{th}^{ch}, and $\Delta\mu_{dr}$ in the compact model (solid black line). Once calibrated, one can depict the individual contribution to ΔI_D by setting the other two parameters to zero. For example, by setting ΔV_{th}^{ch} and $\Delta\mu_{dr}$ to zero, the pure ΔI_D from $\Delta\mu_{ch}$ along with the measured V_G (solid red line) can be plotted. Similar curves can be obtained for the other two components. Interestingly, it shows that a positive shift of ΔV_{th}^{ch} (in V) only causes ΔI_D in the subthreshold region (solid green line). This decomposition explains the reasons for the double peaks. *The first peak in the subthreshold region* $[V_{G(m)} < V_{th}]$ *is due to the exponential dependence on* V_{th}, *which drops dramatically (solid green line) and is taken over by the mobility degradations after* $V_{G(m)} > V_{th}$; *hence, the second peak appears with a valley in the middle*. Furthermore, the traditional HCD metric, $\Delta I_{D,lin}$, adds up their impacts (with weighting factors) of mobility degradation in both regions. Furthermore, the subthreshold region ($\Delta I_{D,sub}$) reveals critical information about channel degradation (which is a combination of $\Delta\mu_{ch}$ and ΔV_{th}^{ch}). The decreasing trend of ΔI_D along measured V_G arises from the feature of $\Delta\mu_{ch}$ (red line in Fig. 3). In essence, the tandem-FET model can be used to fit the degraded I–V characteristics to extract the corresponding $\Delta\mu_{ch}$ (%), $\Delta\mu_{dr}$ (%), and ΔV_{th}^{ch} (V) at any stress time t. The investigation of the subthreshold region allows us to deconvolve the three components (namely, $\Delta\mu_{ch}$, ΔV_{th}^{ch}, and $\Delta\mu_{dr}$). The detailed fitting results on the I–V spectrum are given in the supplementary material. The benefits of matching the degradation spectrum instead of the original I–V curves are as follows: (a) the device-to-device pre-stress I–V variation is not a concern because one obtains $\Delta\mu$(%) directly from ΔI_D(%); (b) it provides the holistic view from off- to on-state in the linear scale. (Semi-log scale for sub- or near-subthreshold matchings is no longer required.)

The need to adapt the full degradation spectrum at each measurement period is time-consuming, and the fitting of the tandem-

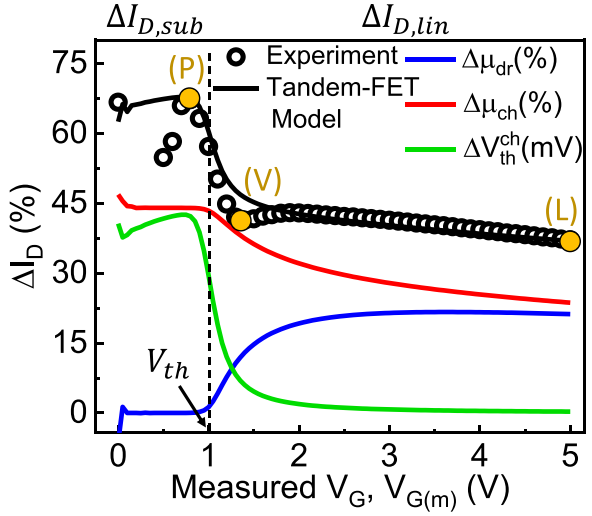

FIG. 3. An example of an I–V degradation spectrum (black circle, under a specific stress condition and after a particular stress time) can be fitted through the tandem-FET model (solid black line). After fitting, the individual impact of the three degradation components on the overall spectrum can be decomposed.

FET model by HSPICE simulation requires expertise in compact modeling. Furthermore, the BSIM6 compact model is complicated, and its use obscures the essential physics of the degradation process. Therefore, based on the insights of the BSIM6 model, we will now derive a three-point analytical model to overcome these shortcomings and directly calculate $\Delta\mu_{ch}$, $\Delta\mu_{dr}$, and ΔV_{th}^{ch}. A detailed analytical derivation of the equations can be found in the supplementary material.

Assuming linear on-state [measured $V_{G(m)} \gg V_{th}^{ch}$, small V_D], the analytical model for the tandem-FET can be derived by interpreting the drift region as a resistor R_{dr}. In the linear region, the drain current with the drift resistance R_{dr} is given by

$$I_D = \frac{\beta_{ch}\left(V_G - V_{th}^{ch}\right)V_D}{1+\beta_{ch}\left(V_G - V_{th}^{ch}\right)R_{dr}} = \frac{I_D^*}{1+K_0}. \tag{2}$$

Here, $\beta_{ch} = \mu_{ch}C_{ox}W/L_{ch}$ and μ_{ch}, W, and L_{ch} are, respectively, the mobility, width, and length of the channel. C_{ox} is the oxide capacitance. Since the drift region is another MOSFET, the drift resistance is given by $R_{dr} = 1/\left(\beta_{dr}(V_G - V_{th}^{dr})\right)$. By definition, $I_D^* \equiv \beta_{ch}(V_G - V_{th}^{ch})V_D$ and $K_0 \equiv \frac{\beta_{ch}(V_G - V_{th}^{ch})}{\beta_{dr}(V_G - V_{th}^{dr})}$. Both terms change after degradations. (K_0' is defined as degraded K_0.)

We can introduce four degradation parameters: M_{ch}, M_{dr}, ΔV_{th}^{ch}, and ΔV_{th}^{dr} to include the mobility degradation multiplier $[M_{(ch,dr)} = \mu_{(ch,dr)}^{deg}/\mu_{(ch,dr)}^{0} < 1]$ and threshold voltage shift [$\Delta V_{th}^{(ch,dr)}$ in V] after HCD. Therefore, the general form of the degraded I_D can be written as

$$I_D^{deg} = \frac{M_{ch}\beta_{ch}\left(V_G - V_{th}^{ch} - \Delta V_{th}^{ch}\right)}{1+\dfrac{M_{ch}\beta_{ch}\left(V_G - V_{th}^{ch} - \Delta V_{th}^{ch}\right)}{M_{dr}\beta_{dr}\left(V_G - V_{th}^{dr} - \Delta V_{th}^{dr}\right)}} = \frac{M_{ch}\beta_{ch}\left(V_G - V_{th}^{ch} - \Delta V_{th}^{ch}\right)}{1+K_0'}. \tag{3}$$

Equation (3) can be further simplified for linear (L) and valley (V) point individually. First, let us start with a **linear point (L)** (on-state). Here, $V_G - V_{th}^{(ch,dr)} \gg \Delta V_{th}^{(ch,dr)}$ so that all $\Delta V_{th}^{(ch,dr)}$ terms are negligible, indicating that degradation depends primarily on the mobility degradation of the two regions (M_{ch} and M_{dr}), but not on $\Delta V_{th}^{(ch,dr)}$, as verified in Fig. 3. From Eqs. (2) and (3),

$$\Delta I_D^{(L)}(\%) \equiv \frac{I_D - I_D^{deg}}{I_D} = \frac{M_{dr}(1-M_{ch}) + K_0 M_{ch}(1-M_{dr})}{M_{dr} + K_0 M_{ch}}. \tag{4}$$

It is worth mentioning that K_0 is an essential parameter for device customization because $K_0 \propto \beta_{ch}/\beta_{dr} \propto L_{dr}/L_{ch}$. For a device with a longer drift region than this specific LDMOS, K_0 will be larger, and $\Delta\mu_{dr}$ will become more pronounced in ΔI_D compared to $\Delta\mu_{ch}$.

The second point to be considered is the **valley point (V)**, as shown in Figs. 1(c) and 3, which occurs slightly (0.1 V is assumed) above V_{th}. Since $V_G - V_{th}^{ch} = V_D = 0.1$, the previous linear drain current [Eq. (2)] needs to be corrected with a factor of 2. The parameter K_0' defined in Eq. (3) now becomes

$$K_0' = \frac{M_{ch}\beta_{ch}/2}{M_{dr}\beta_{dr}}\frac{\left(0.1 - \Delta V_{th}^{ch}\right)}{\left(1.1 - \Delta V_{th}^{dr}\right)} \approx \frac{M_{ch}}{M_{dr}}\frac{\beta_{ch}}{\beta_{dr}}\frac{\left(0.1 - \Delta V_{th}^{ch}\right)}{2.2}. \tag{5}$$

Revised Eq. (3) gives $I_D^{\deg} = \frac{M_{ch} I_D^*/2}{1+K_0'}$. Near V_{th}, $K_0 \ll 1$ and, hence, $I_D \approx I_D^*/2$. $\Delta I_D^{(V)}(\%)$ can, therefore, be written as

$$\Delta I_D^{(V)}(\%) \equiv \frac{I_D - I_D^{\deg}}{I_D} = 1 - \frac{M_{ch}}{1+K_0'}. \quad (6)$$

We may further simplify it because K_0' is less than 0.1. By applying $(1+K_0')^{-1} \approx 1 - K_0'$, we can write

$$\Delta I_D^{(V)}(\%) \approx 1 - M_{ch}(1-K_0') = (1-M_{ch}) + \frac{M_{ch}^2}{M_{dr}}\frac{\beta_{ch}}{\beta_{dr}}\frac{(0.1-\Delta V_{th}^{ch})}{2.2} \approx 1 - M_{ch}. \quad (7)$$

One can either choose to adopt Eq. (6) as an exact form or use Eq. (7) for a quick estimate.

Finally, let us consider the **peak point (P)** in the subthreshold region. At this point, the subthreshold current, $I_{D,sub} = I_S \exp\left(\frac{q(V_G - V_{th})}{mkT}\right)$, where $I_S(\propto \mu)$ is a constant at fixed V_D, kT/q is the thermal energy at ambient temperature, and m is the body coefficient. The degradation of the channel mobility degrades I_S, while ΔV_{th} degrades $I_{D,sub}$ exponentially. Therefore,

$$\Delta I_D^{(P)}(\%) \equiv \frac{I_D - I_D^{\deg}}{I_D} = 1 - M_{ch} \exp\left(\frac{-\Delta V_{th}^{ch}}{mkT/q}\right). \quad (8)$$

For the case $\frac{\Delta V_{th}^{ch}}{mkT/q} \ll 1$, Eq. (8) can be further simplified with Taylor's expansion of the exponential term ($e^{-x} \approx 1 - x$),

$$\Delta I_D^{(P)}(\%) \approx (1 - M_{ch}) + M_{ch}\frac{\Delta V_{th}^{ch}}{mkT/q}. \quad (9)$$

Since $mkT/q \sim 52$ mV at room temperature, Eq. (9) works well for relatively small ΔV_{th}^{ch}. As predicted in Fig. 3, both the channel mobility and threshold voltage degradation could contribute to $\Delta I_{D,sub}$. Given these three unique points (i.e., P, V, and L), Eqs. (4), (5)–(7), and (8) and (9) allow us to directly and intuitively calculate the three unknowns, $\Delta\mu_{ch}$, $\Delta\mu_{dr}$, and ΔV_{th}^{ch}.

Figure 4(a) shows that this Peak–Valley–Linear (PVL) algorithm (symbols) reproduces $\Delta\mu_{ch,dr}$ obtained by fitting the full degradation spectrum with the BSIM6-based tandem-FET compact model (lines). It is noteworthy that when $\Delta\mu < 1\%$; the compact model cannot be precisely fitted due to the weak/noisy ΔI_D peak. In this regime, the analytical approach [Eqs. (4)–(9)] offers a more accurate and much faster calculation of mobility degradation. For higher degradation ($\Delta\mu > 1\%$), the three-point analytical technique and a tandem-FET compact model give comparable results, as expected. Note that the linear relationship in a log–log plot implies that $\Delta\mu_{ch,dr}$ follows a power-law degradation.

Figure 4(b) shows $\Delta I_D^{(P)}(\%)$ vs ΔV_{th}^{ch} (mV) from experiments, where its linear behavior is suggested by Eq. (9). It deviates from the linear curve at higher ΔV_{th}^{ch} as expected (works well when $\Delta V_{th}^{ch} < 15$ mV). The smaller slope of $V_{G(s)}/V_{D(s)} = 4$ V/8 V case is due to the higher calculated $\Delta\mu_{ch}(\%)$ (smaller M_{ch}). In both cases, channel degradation is minor, $M_{ch} \lesssim 1$, so that the offset term in Eq. (9), $1 - M_{ch} \approx 0$. Here, the coefficient, $m \approx 2$, justifies the derivations.

Finally, the time kinetics of deconvoluted $\Delta\mu_{ch}$ and $\Delta\mu_{dr}$ under different stress conditions are compared. Figure 5(a) shows an increasing $\Delta\mu_{ch}$ and decreasing time exponent (0.5 to 0.2), whereas $\Delta\mu_{dr}$ does not vary for different stress $V_{G(s)}$, with a smaller time exponent around 0.1. Similar results have been reported in other papers.[17,18] Figure 5(b) replots the data in Fig. 5(a) to compare the degradations at the final stress time. The results agree well with the generation of interface trap (ΔN_{it}) extracted through CP-related technique.[11] LDMOS transistors for different applications can have distinct structures, geometries, and doping levels. For example, an LDMOS with field oxide, depending on the stress condition, may have three hotspots, and only two of them contribute to overall ΔI_D.[19] Therefore, although the concept of three-point I–V spectroscopy was demonstrated on one specific structure in this paper as a prototype, it holds for LDMOS transistors with different drift lengths and doping configurations. The general principle proposed (e.g., representing a transistor into a set of sub-transistors, determining the critical points on the I_D–V_G curve that localizes the degradation associated with individual sub-transistors, and extracting the degradation parameters related to the critical points) can be a versatile approach for the degradation characterization of other configurations of the LDMOS transistor as well. Although in most LDMOS transistors, the features of the I–V spectroscopy (first peak in subthreshold, then a valley near the threshold, and a peak again after the threshold) are similar, this model should also be applicable in devices

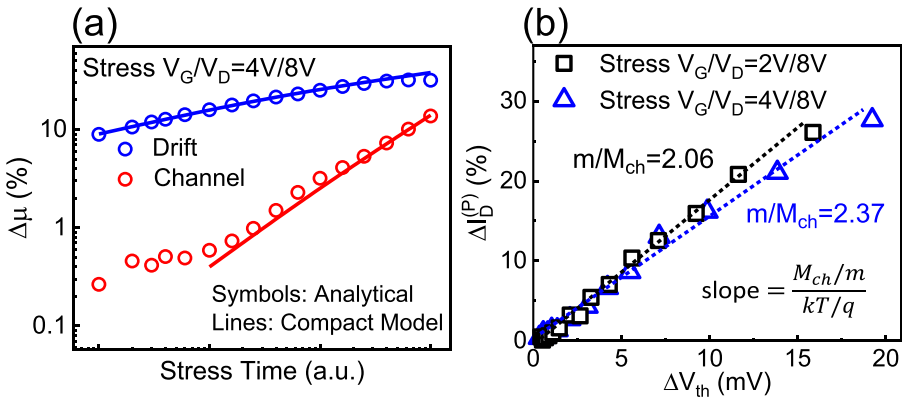

FIG. 4. (a) The comparison of $\Delta\mu(t)$ in the log–log scale between the compact model and the analytical model (stress condition: $V_G/V_D = 4$ V/8 V as an example). (b) Verification of the relation of $\Delta I_D^{(P)}$ and channel ΔV_{th} from Eq. (9).

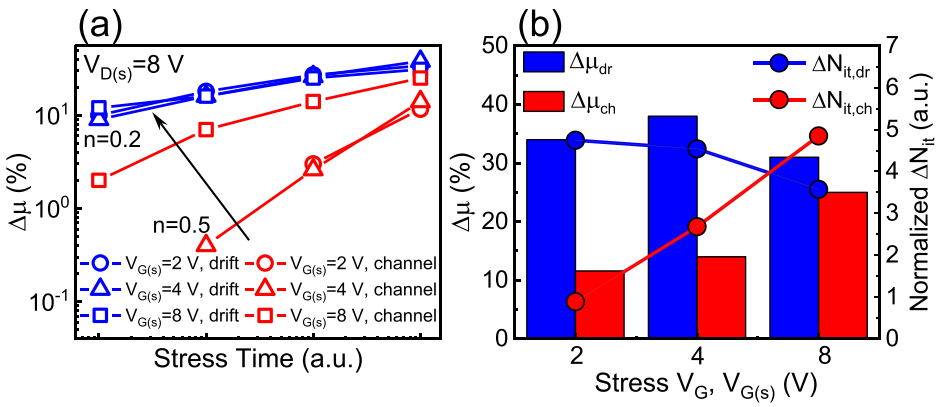

FIG. 5. (a) The extracted channel and drift $\Delta\mu(t)$ at various stress conditions. (b) Comparison of extracted $\Delta\mu$ to ΔN_{it} extracted from technique[11] at final stress time.

where the peak and the valley may not be easily distinguishable. In those cases, any point in the subthreshold region can be chosen as (P), and any point close to the threshold can be chosen as (V) to perform the analysis.

In conclusion, using an n-channel LDMOS as an example, the three-point I–V spectroscopy technique is proposed as a powerful HCD characterization approach. It unveils the degradation components without conducting detailed, and time-consuming characterization of multiple degraded spots using the charge pumping technique. The physics underneath its double-peak feature is fully explored through the proposed tandem-FET model. Those deconvoluted degradation parameters ($\Delta\mu_{ch}$, $\Delta\mu_{dr}$, and ΔV_{th}^{ch}) can be obtained by either fitting the BSIM6-based compact model or solving the derived three-point analytical model (results are comparable). The general principle of using a physics-based compact model to derive a device-specific characterization protocol should generalize to other power transistors as well.

See the supplementary material for the detailed calibrations of the tandem-FET compact model, fitting of the I–V spectroscopy, the detailed derivations, and justifications of the analytical model.

AUTHORS' CONTRIBUTIONS

Y.-P.C and B.K.M contributed equally to this work.

The authors gratefully acknowledge the access to the characterization facilities at Birck Nanotechnology Center, Purdue University, for the results presented in this article.

The authors declare no competing financial interest.

DATA AVAILABILITY

The data that support the findings of this study are available from the corresponding author upon reasonable request.

REFERENCES

[1]M. Saremi, M. Saremi, H. Niazi, M. Saremi, and A. Y. Goharrizi, J. Electron. Mater. **46**, 5570 (2017).
[2]M. Saremi, B. Ebrahimi, A. Afzali-Kusha, and S. Mohammadi, Microelectron. Reliab. **51**, 2069 (2011).
[3]S. Mahapatra, D. Saha, D. Varghese, and P. B. Kumar, IEEE Trans. Electron Devices **53**, 1583 (2006).
[4]Y. Chen, B. K. Mahajan, D. Varghese, S. Krishnan, V. Reddy, and M. A. Alam, "A novel 'I-V Spectroscopy' technique to deconvolve threshold voltage and mobility degradation in LDMOS transistors," in *2020 IEEE International Reliability Physics Symposium (IRPS)* (2020), pp. 1–6.
[5]M. A. Alam, B. K. Mahajan, Y.-P. Chen, W. Ahn, H. Jiang, and S. H. Shin, IEEE Trans. Electron Devices **66**, 4556 (2019).
[6]M. A. Alam, B. K. Mahajan, and Y.-P. Chen, "Hot carrier degradation in classical and emerging logic and power electronic devices: Rethinking reliability for next-generation electronics," in *5th IEEE Electron Devices Technology and Manufacturing Conference* (EDTM) (IEEE, 2021), pp. 1–3.
[7]B. K. Mahajan, Y.-P. Chen, and M. A. Alam, IEEE Trans. Electron Devices **68**, 3923 (2021).
[8]A. N. Tallarico, S. Reggiani, R. Depetro, S. Manzini, A. M. Torti, G. Croce, E. Sangiorgi, and C. Fiegna, IEEE Trans. Electron Devices **65**, 5195 (2018).
[9]H. Tahi, B. Djezzar, and B. Nadji, IEEE Trans. Electron Devices **57**, 2892 (2010).
[10]C. C. Cheng, K. C. Tu, T. Wang, T. H. Hsieh, J. T. Tzeng, Y. C. Jong, R. S. Liou, S. C. Pan, and S. L. Hsu, "Investigation of hot carrier degradation modes in LDMOS by using a novel three-region charge pumping technique," *2006 IEEE International Reliability Physics Symposium Proceedings* (2006), pp. 334–337.
[11]Y. P. Chen, B. K. Mahajan, D. Varghese, S. Krishnan, V. Reddy, and M. A. Alam, IEEE Trans. Electron Devices **68**, 726 (2021).
[12]B. K. Mahajan, Y.-P. Chen, D. Varghese, S. Krishnan, V. Reddy, S. Krishnan, and M. A. Alam, "Quantifying region-specific hot carrier degradation in LDMOS transistors using a novel charge pumping technique," in *2021 IEEE International Reliability Physics Symposium (IRPS)* (2021), pp. 1–6.
[13]C. L. Lou, W. K. Chim, D. S. H. Chan, and Y. Pan, IEEE Trans. Electron Devices **45**, 1317 (1998).
[14]S. Reggiani, S. Poli, M. Denison, E. Gnani, A. Gnudi, G. Baccarani, S. Pendharkar, and R. Wise, IEEE Trans. Electron Devices **58**, 3072 (2011).
[15]A. Ortiz-Conde, F. J. García Sánchez, J. J. Liou, A. Cerdeira, M. Estrada, and Y. Yue, Microelectron. Reliab. **42**, 583–596 (2002).
[16]H. Agarwal, C. Gupta, P. Kushwaha, C. Yadav, J. P. Duarte, S. Khandelwal, and C. Hu, "Analytical modeling and experimental validation of threshold voltage in BSIM6 MOSFET model," IEEE J. Electron Dev. Soc. **3**(3), 240–243 (2015).
[17]P. Moens, J. Mertens, F. Bauwens, P. Joris, W. De Ceuninck, and M. Tack, "A comprehensive model for hot carrier degradation in LDMOS transistors," in *Proceedings of the 45th Annual IEEE International Reliability Physics Symposium* (IEEE, Phoenix, AZ, 2007), pp. 492–497.
[18]A. N. Tallarico, S. Reggiani, R. Depetro, A. M. Torti, G. Croce, E. Sangiorgi, and C. Fiegna, IEEE J. Electron Devices Soc. **6**, 219 (2018).
[19]P. Moens, F. Bauwens, and M. Thomason, "Two-stage hot carrier degradation of LDMOS transistors," in *Proceedings. ISPSD '05. The 17th International Symposium on Power Semiconductor Devices and ICs, 2005* (IEEE, 2005), pp. 323–326.